Journal of The Electrochemical Society, 2023 **170** 072505
1945-7111/2023/170(7)/072505/13/$40.00 © 2023 The Electrochemical Society ("ECS"). Published on behalf of ECS by IOP Publishing Limited

Quality and Efficiency Control of Electrodeposition and Electrodissolution of Ni on a Ternary Composite Electrode Followed by Digital Video Electrochemistry

Jerónimo Agrisuelas, José J. García-Jareño,[z] Manuel Piedras, and Francisco Vicente*

Physical Chemistry Department, University of Valencia, 46100 Burjassot, Spain

The quality of metal electrodeposits on different surfaces depends on the configuration and composition of the electrochemical bath, but also on the control of experimental variables that can affect the electrode processes taking place. In this work, we have studied the electrodeposit of nickel on a polypropylene|graphite|copper (PP|G|Cu) ternary composite electrode. Together with the resistive behavior of the electrode, the nickel electrodeposition presents extra difficulties as a low reduction potential and numerous and possible chemical reactions with the medium to form passive layers or aqueous complexes. The use of digital video electrochemistry (DVEC) has allowed detecting some issues during the electrodeposition and electrodissolution processes such as the non-uniform growth of Ni due to the electrode configuration, secondary and oscillatory electrochemical reactions caused by the subproducts in the auxiliary electrode or the effect of the formation of hydrogen bubbles. The estimation of electrodeposition efficiency from DVEC and a possible electrodissolution mechanism are discussed.
 [DOI: 10.1149/1945-7111/ace4f6]

Manuscript submitted May 10, 2023; revised manuscript received June 26, 2023. Published July 14, 2023.

Electroplating is an industrial process which produces a high-quality surface, usually a metal, on the surface of a conductive substrate with the purpose of aesthetically improving the appearance of the substrate or conferring new properties for technological applications. Despite this improvement, this process requires significant electricity consumption and the use of additives to improve and to optimize this process. Due to the low reduction potentials of some metals, electroplating often takes place together with parallel reactions such as hydrogen evolution (HER) causing a decrease in electrical efficiency and a loss in the aesthetic quality of the final product. This is why the metallurgical industry requires strategies to minimize the use of energy, but also to reduce the use of additives and raw materials in general, which make the final product more expensive, but also represent an environmental problem.[1–3] Despite these problems, the electroplating process makes it possible to obtain a low-cost material with the surface properties of a technological metal. If the electroplating process takes place on carbon-based composite materials allows increasing the surface area of the material, which improves its properties as a possible electrode for electrocatalysis. Conducting composite materials have attracted a large interest during the last years due to their good mechanical properties, low weight, easiness to be conformed and their possible use as electrodes in different technological applications.[4–6] Most of these conducting composite materials are obtained by dispersing carbonous conducting particles such as graphite, carbon nanotubes, carbon nanofibers or graphene in a polymer matrix.[7–10] Conductivity of these materials increases with the amount of conducting particles dispersed in, but it could result in fragile and easy to broke materials.[8,11,12] In recent years, ternary composite materials have been tested improving the hardness and quality of the composite material for different uses. These materials are fabricated by introducing metal-compound particles together with carbonous particles and the polymeric matrix, reducing the amount of carbonous particles and increasing the consistence of the material.[8,13–17]

The surface of the resulting material shows a dark color characteristic for the carbonaceous particles. In a recent publication, we have tested the possibility to cover the polypropylene|graphite| copper (PP|G|Cu) ternary composite with a thin layer of Cu by electroplating.[17,18] When it is necessary to cover an inhomogeneous conductive surface with a metal, a series of difficulties arise that must be solved for an optimal final product. On the one hand, the coating must completely cover the surface of the base material, on the other hand, this coating should be as homogeneous as possible to also achieve with a smaller amount of metal the best result. The non-homogeneity of a surface can be due to several factors: electrical resistance of the material, roughness or porosity, geometric arrangement of the electrodes in the electrochemical cell, etc. These factors can cause the coating to be carried out preferably on some parts of the surface, increasing the economic cost of the industrial process or creating unwanted products.

Focusing now in this research, *Ni* electroplating is a more complex process than *Cu* electroplating.[19] Electrodeposition of *Ni* takes place at more cathodic potentials than electrodeposition of *Cu* and some secondary chemical or electrochemical reactions could occur. The most important reaction is HER during *Ni* electroplating which decreases the electrochemical reaction efficiency since a part of the energy is lost reducing the hydronium cations. In addition, there is the formation of bubbles on the electrode surface which hinder the metal deposition on the region under the bubble. Another difficulty is that the relative high resistance of the composite material before electrodeposition makes the deposit to grow following a directional trend along the electrode from lower resistance regions to higher resistance regions obtaining a final product with a non-homogeneous thickness.[17,18]

The *Ni* surface reactions in different media can also affect the quality and the amount of the electroplated surface. Passive layers can grow on the *Ni* metal surface due to their high reactivity and the nature of these passive layers is highly dependent on the pH of the electroplating solution.[20–24] Finally, there is the electrical resistance of the electroplating solution and the relative position of electrodes in the electrochemical cell which can cause non-ideal effects.[25] If electrodes were near enough, the ohmic drop of the solution was minimized but subproducts on the auxiliary electrode can reach the working electrode interfering in the electrochemical Ni^{2+} reduction.[26]

In this research, the quality of the *Ni* electroplated surface on the PP|G|Cu electrode has been followed in situ by digital video-electrochemistry (DVEC). Here, we assay different configurations for the electrodeposit of *Ni* on a 1x1 cm of this resistive composite material. The aim of this work is not only to obtain a high-quality electrodeposit, but also, we try to detect different problems during an electroplating process by the analysis of DVEC procedures.

DVEC has revealed as a non-expensive solution for the control of electrodeposition processes on different kind of surfaces as explained elsewhere.[17,27] This technique consists basically in recording the digital video of the electrode surface during the electrochemical experiment. Then, video is separated into individual frames each

*Electrochemical Society Member.
[z]E-mail: Jose.J.Garcia@uv.es

time interval. DVEC takes advantage of a fast CCD sensor recording the video of the electrode surface during the electrochemical processes. Usually, a digital camera gets video at different resolutions and at 30 frames per second. If color images are analyzed, each photogram can be represented as 3 different matrixes of pixels, one per each color coordinate RGB (Red, Green and Blue). Each pixel is characterized by their color intensities, I_R, I_G and I_B. Two statistical parameters were used to summarize all the information of each photogram in a picture with a defined number of pixels n_{pixels}. On the one side, there is the mean color intensity ($\bar{I}_{RGB}$) for each color coordinate evaluated as:

$$\bar{I}_{RGB} = \sum_{j=1}^{n_{pixel}} \frac{I_{RGB}(j)}{n_{pixels}} \quad [1]$$

This first parameter can measure the amount of electroactive and colored species on the selected electrode surface, a second parameter measuring the color dispersion can help for the analysis of the surface homogeneity. This is the standard deviation or variance, sd^2_{RGB}, which can be easily related with kinetic parameters of the electrochemical process.[28,29] The variance can be evaluated as:

$$sd^2_{RGB} = \frac{\sum_{j=1}^{n_{pixels}} (I_{RGB}(j) - \bar{I}_{RGB})^2}{n_{pixels}} \quad [2]$$

If the surface proves homogeneous enough, this parameter should reach very low values but for a non-homogenous surface, higher values should be expected. During the change of the electrode surface from a homogenous color to a different homogenous covered surface (electroplated surface) a maximum should be observed if ½ of the electrode surface is covered and the other ½ uncovered.[28,30] That makes of variance a very interesting parameter for evaluating kinetics of electrochemical processes since this maximum proves a measurement of the half-life time for different processes. The resolution of this technique allows to distinguish (for 8 bit images) up to 2^{24} colors and for each RGB coordinate we have 256 color levels, ranging from no color (black,0) to pure color (255). The resolution increases when analyzing a set of pixels, since for an image of 100 × 100 pixels an average value of 10000 pixels is calculated and we can detect average intensity changes of one hundredth of an RGB unit. Although the classical spectroscopy shows more and precise resolution, Digital analysis of images allows characterizing in a fast way the quality and homogeneity of the plated or electroplated surfaces, but also the covering rate of the composite material or the presence of different intermediate species or bubbles on the electrode surface.[17]

As in spectroscopy, flat, equally illuminated and smooth surfaces are preferred to obtain good results However, the measurement of color variance is also a good measure of the irregularities and inhomogeneities on the surface and on the other hand, images of curved surfaces may have shadowing. This can be partly overcome by the use of lenses or different light sources. In addition, the technique allows the analysis of a particular region of the surface and to follow its independent evolution over time. It is also possible to take images simultaneously from different angles to partially overcome these shortcomings.

Together with nickel electrodeposition, in this work we want to evaluate the use of DVEC as a fast and non-expensive tool to detect different problems during the electroplating process, in order to be able to correct them in situ. For that, we describe some of these issues and try to solve them. The spatiotemporal analysis is one of the most important advantages of DVEC during surface changes. The great capacity of computer systems for data analysis and the possibility to acquire simultaneously a large amount of information of different variables and during a time interval allows the spatiotemporal data analysis to reveal as a promising procedure for the optimization of different processes. Spatiotemporal data analysis has been used in different fields, among them, climate environments change, surface kinetics changes or population distribution. This term refers to the analysis of different data with time attributes and absolute and relative positions in a 3D space, as well as the process and methodology of analyzing these data.[27,31,32] Among the aims of this manuscript, there is also proving the goodness of the spatio-temporal data analysis for the optimization of several electroplating processes.

Image analysis for the quality control of electroplated surfaces is not new, but this control is usually made after the electroplated surface was generated.[33,34] The use of DVEC allows recording the quality of the electrogenerated layer at any time during the electroplating process or even, for recovery purposes during the metal electrodissolution. These facts prove of special interest for evaluating kinetics and optimizing the experimental setup and conditions. For the quantitative description of the electrochemical behavior of these processes, the image analysis recently developed and explained in [28,29] are absolutely necessary for a correct interpretation.

Experimental

The electrochemical cell was a two electrodes cell working in a galvanostatic mode. The working electrode was a ternary composite material with 50% Polypropylene, 40% graphite and 10% Cu randomly dispersed provided by AIMPLAS (PP|G|Cu electrode). The size of the electrode was a 2 × 1 cm rectangle. The copper wire is connected to the electrode with silver paint, to ensure a good electrical contact, and it is reinforced with epoxy adhesive (Poxipol™). The back side of the electrode and laterals were covered with epoxy resin to assure that the reaction only takes place on the front side of the electrode. Finally, the electrode was covered with Teflon tape leaving about a 1 × 1 cm of active surface area uncovered. Figure 1 shows an image of both sides of the working electrode.

All the experiments were galvanostatic and controlled by a potentiostat-galvanostat PAR 273, the auxiliary electrode was a large area Pt mesh, the electrochemical cell was a transparent Hellma optical glass (25 × 25 mm optical path length). For the *Ni* electrodeposition a 245 mM K_2SO_4, 5 mM H_2SO_4 and 100 mM $NiSO_4$ solution was used[35] and a current of −4 mA for 7200 s was applied. The electrodeposition takes place by the reduction of Ni^{2+}_{aq} to *Ni* on the electrode surface.

For the *Ni* electrodissolution experiments, a controlled current of + 4 mA was applied during the necessary time to obtain the naked electrode surface. This experiment was carried out in a 10 mM H_2SO_4 and 245 mM K_2SO_4 or in a 1 mM HCl and 210 mM KCl solution. For the vibrating electrode experiments a 11000 rpm 1020 flat coin button-type micro DC vibrating was coupled to the working electrode removing the bubbles on the electrode and allowing the Ni^{2+} cations to reach the electrode surface.

The video of the electrode surface was registered during all the experiments with the help of a digital camera (EPA-503278) under light controlled conditions (15 W, LED lamp 6500 K white cold light). Video was analyzed with the help of a home-made software that extracts photograms to individual images. After this, a selected region of the electrode surface was analyzed obtaining the mean color intensities ($\bar{I}_{RGB}$) for all three coordinates (Red, Green and Blue) and the standard deviation (variance, sd^2_{RGB}) of color intensities.[18] For the 3D plots, the time evolution of the electrode surface was simultaneously analyzed at different regions covering the whole electrode surface.[17]

Results and Discussion

We start with the electrochemical response and mean color intensities evolution during the electroplating experiment, then we analyze the variance of color intensities as a measurement of the color dispersion.

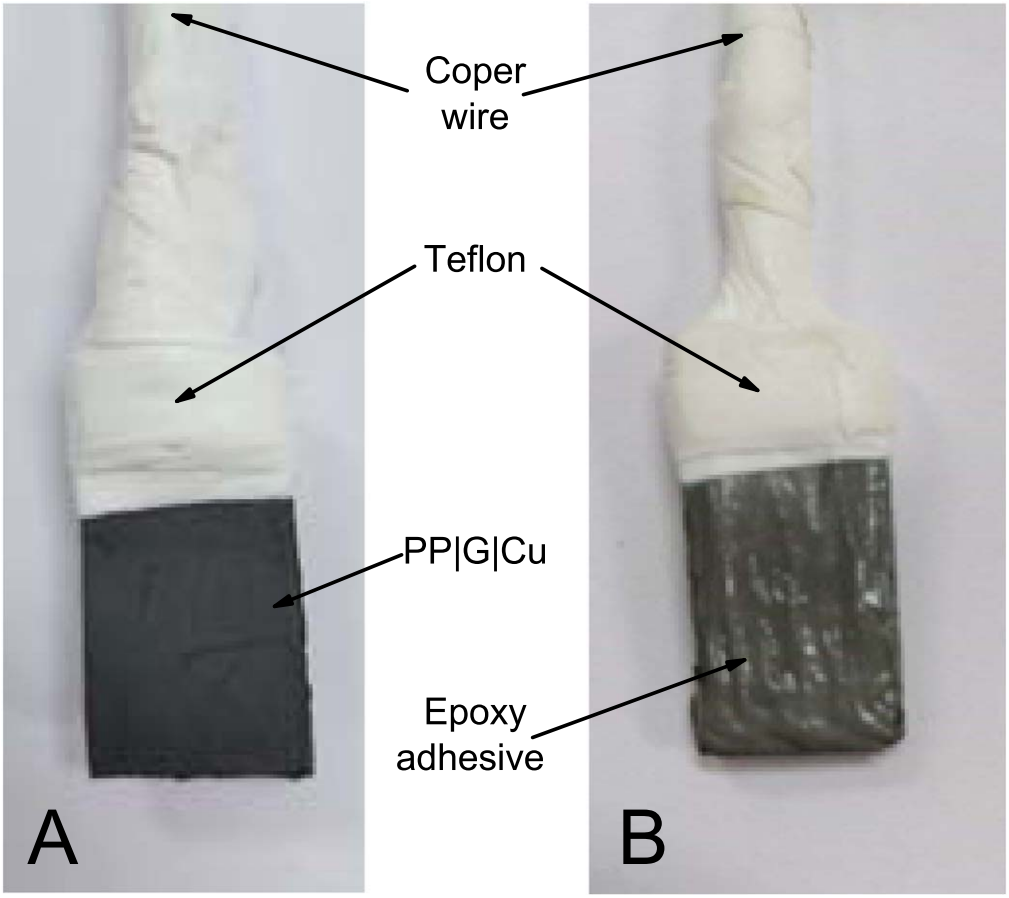

Figure 1. Front side (A) and back side (B) of the working PP|G|Cu ternary electrode. The back side was covered with an insulating epoxy resin.

Electrode configuration in the electrochemical cell.—It is well known that the transport of electroactive species can control the rate of an electrochemical process. In an electrochemical cell the current flows between the working electrode and the auxiliary electrode. If both electrodes are far apart, the uncompensated resistance can be high, increasing the energy losses due to the Joule effect. However, if electrodes are too close, by-products from the auxiliary electrode can reach the surface of the working electrode and interfere with the overall reaction.[26,36]

Narrowly separated electrodes.—Figures 2A and 2B show the time evolution of potential and mean color intensities of the electrode surface during a galvanostatic procedure of *Ni* electrodeposition where the auxiliary and the working electrodes were only shortly separated (about 0.5 cm). Whereas the potential reaches an almost constant value around −2.8 V after a few seconds of current application, RGB mean color intensities increase as the *Ni* is deposited on the right side of the composite electrode, the part closest to the auxiliary electrode (see images in Fig. 2A). An oscillatory response in both, potential and color intensity curves, is recorded. This behavior can be explained by the fact that radical species formed on the auxiliary electrode can react with the species in the medium which finally can oxidize the small amount of *Ni* electrodeposited on the working electrode.[37,38] In the electrochemical cell, current flows between the auxiliary and working electrodes. In galvanostatic mode, when a reduction current is forced on the working electrode, this necessarily involves oxidation processes on the auxiliary electrode. The greater this current the greater the overpotential at the auxiliary electrode to achieve this current and that means the production of these radical species. This behavior has also been observed during *Cu* electrodeposition in a SO_4^{2-} containing solution[26] or during the dissolution of *Co* in acid solutions containing Cl^- anions.[36] The time evolution of variance also shows this oscillatory behavior (Fig. 2C).

A model explaining the oscillatory behavior has been recently proposed for the *Cu* electrodeposition studies.[26,37,38] Scheme 1 shows a similar and simplified mechanism which can explain the *Ni* oscillatory electrodeposition. During the first 4000 s, the time interval where oscillations appear, there is only a small amount of *Ni* deposited on the electrode. After 4000 s, the oscillations are damped and *Ni* begins to be observed on the right side of the electrode. Since the small distance to the working electrode is proposed to be the cause of this oscillatory behavior, two regions of the electrode have separately been studied, one marked as right (close to the aux electrode) and the other as left (far from the aux electrode). Figure 2B clearly shows that the color intensity oscillations have a higher amplitude on the right side than on the left side. However, we do not observe any temporal shift in the oscillations between the right and left side. One possible explanation is that the different amplitude is caused by the fact that, due to the proximity to the auxiliary electrode, there is a lower electrical resistance between this part of the electrode and the auxiliary electrode and hence a higher current flows.

As for the temporal coincidence, these images have been acquired at a rate of 1 image each 3 s and differences between the left and right side of the electrode should be very much smaller.

These facts proved that the electrode disposition in the electrochemical cell is a key factor in the quality and homogeneity of the electrode covering. This non-homogeneous layer growth can be solved if both electrodes were more separated or placing a membrane between them avoiding that subproducts on the auxiliary electrode can reach the working electrode.[26]

Figure 2C shows the time evolution of variance of color intensities during this experiment. When the whole surface is

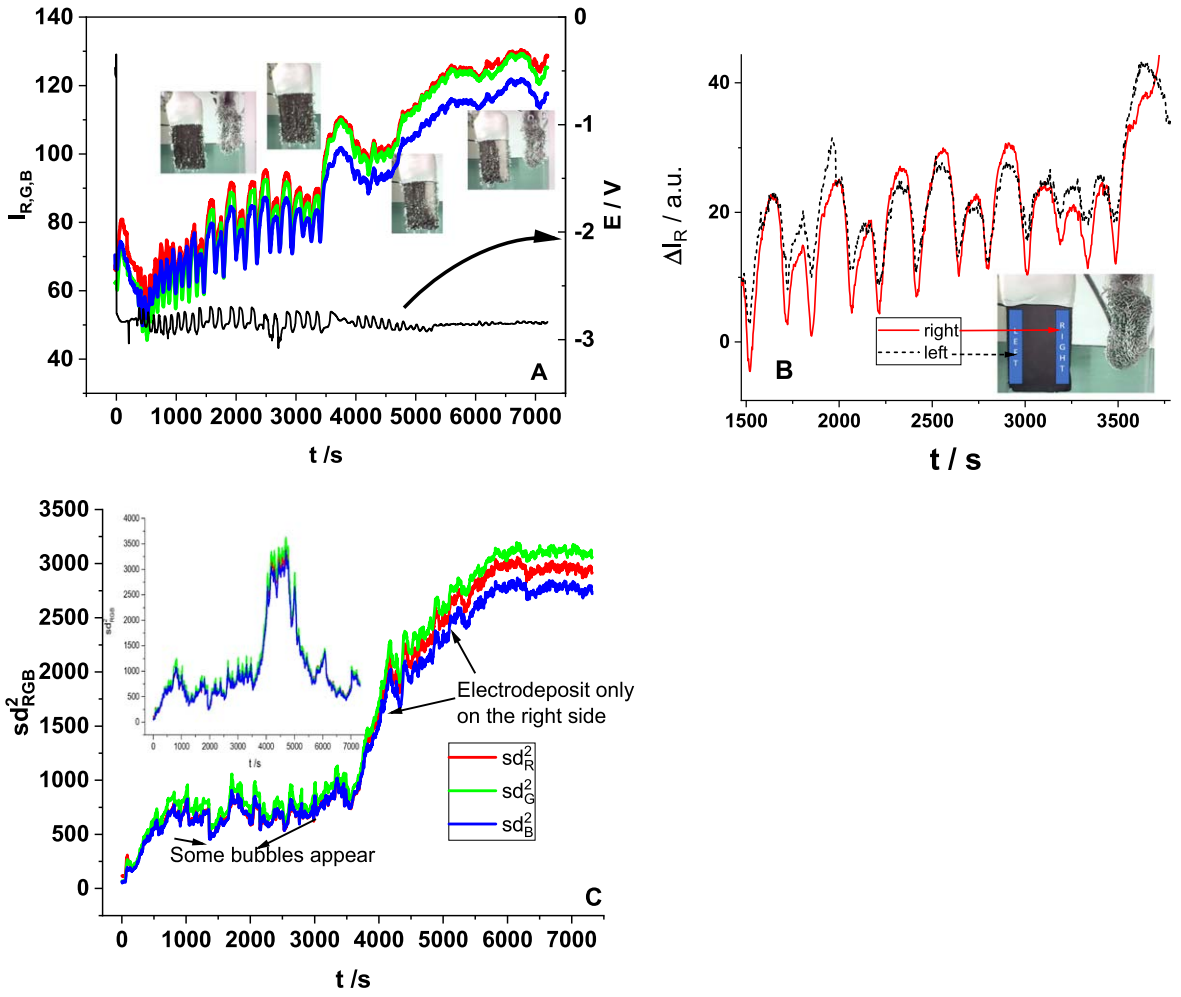

Figure 2. Electrodeposition of Ni without vibration. Galvanostatic experiment with a controlled current of −4 mA in a 245 mM K_2SO_4, 5 mM H_2SO_4 and 100 mM $NiSO_4$ aqueous solution. (A) shows the time evolution of mean color intensities and the measured potential; (B) shows the time evolution of the red color intensity in the time range between 1500 s and 3500 s on two regions on the electrode (left and right). (C) shows the time evolution of the mean color variance during the experiment. Inset of (C) represents the variance changes on the right side of the electrode. Auxiliary electrode was around 0.5 cm on the right of the working electrode.

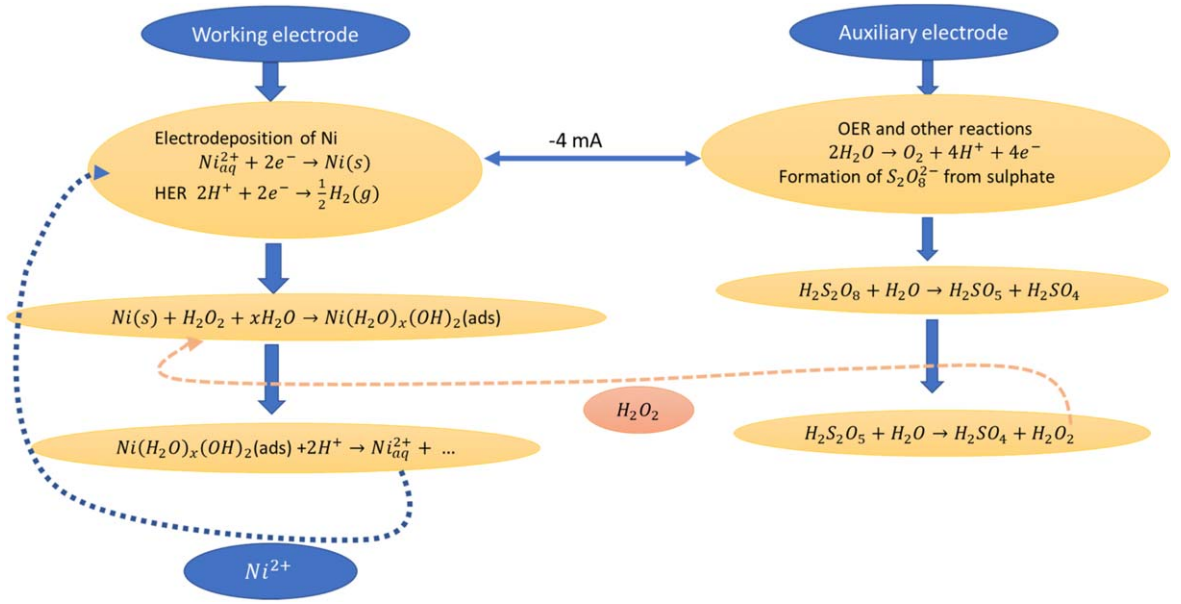

Scheme 1. Simplified schema explaining the redissolution of freshly deposited Ni if electrodes are near enough.[26,37,38]

analyzed, we observe a first increase arriving at a plateau due to the formation of bubbles on the electrode surface, since these bubbles are detected as inhomogeneities of the electrode surface. After 4000 s the variance growths faster indicating that a part of the electrode surface was covered by *Ni*, arriving at a new and higher plateau. There is no decrease in variance since for these times and considering the entire electrode surface, less than ½ of the electrodes was covered by *Ni*. These observations are fully compatible with the mean color intensities evolution. Ideally during an electroplating experiment, the variance of color intensities should change from a minimum value when the composite electrode is bared to a maximum value when ½ of the electrode surface is covered and finally decreasing up to a new minimum if the entire surface is covered by the metal[17,28] If only the right side of the electrode, where nickel is deposited, is analyzed the experimental evolution of variance approximates to the ideal behavior reaching the half of the electrode surface covered by nickel around 4500 s (inset of Fig. 2C). This is one of the main advantages of DVEC, allowing both a global analysis but also the analysis of a small portion of the electrode.

Bubbles on the electrode surface during the electrodeposition of Fig. 2 mean that hydrogen evolution reaction (HER) is taking place simultaneously with the Ni^{2+} reduction to *Ni* causing an important decrease of the electrical efficiency of electrodeposition.[39] Furthermore, the presence of bubbles on the composite surface represents another problem to be solved since bubbles does not allow Ni^{2+} cations to approach to the electrode surface, and then, no electrodeposition takes place where H_2 bubbles appear. In addition, these bubbles also affect the quality and aesthetic appearance of the electrodeposit. DVEC has made it possible to detect this process from 500 s of galvanostatic electrodeposition on the basis of the increase in the color variance of the electrode surface.

Widely separated electrodes.—One of the solutions to the problem of oscillations is to sufficiently separate the electrodes in the cell. Thus, the highly reactive radicals formed at the auxiliary electrode do not reach the nickel electrodeposit. In this experiment we place the auxiliary electrode behind the working electrode and at a distance of 1.2 cm (Fig. 3A). The potential measured during the experiment shows jumps, but no oscillatory behavior as when the electrodes were in close proximity. On the other hand, the color intensity increases during the first few seconds, but reaches a constant value that is maintained for 3500 s. In this case, the electrodeposition process showed a non-homogeneous growth and a very small efficiency. After 3500 s, there is only a small amount of *Ni* on the electrode surface and the most of *Ni* metal was located on the bottom of the electrode. We can explain this result considering the relative disposition of the electrodes. Thus, the preferred site of growth is the bottom of the working electrode, the electrode region closer to the auxiliary electrode.

The initial increase in color intensity on the electrode is explained by the formation of hydrogen bubbles that make the electrode surface appear lighter. However, after the bubbles are formed and as these bubbles were not removed from the electrode surface, the color intensity does not change. After 3500 s these bubbles were mechanically removed from the electrode by shaking it, this causes the increase in color intensity since the *Ni* layer starts growing more homogeneously. At times larger than 5000 s, the *Ni* layer continues growing but there is no color change since all the surface was electroplated and therefore *Ni* is deposited on the previously deposited layer. Noise in Fig. 3 is caused by the appearance and mechanical removal of H_2 bubbles formed on the electrode surface.

In those concerning the variance analysis (Fig. 3B, a first increase of variance by the presence of bubbles is measured, then variance also increases due to the *Ni* electrodeposition and after, when more than one half of the electrode surface was covered by *Ni*, there is a decrease until the electrode was fully covered by *Ni*. Finally, since *Ni* grows on previously deposited *Ni* there is no color change, and the variance also keeps constant, even if electrodeposition continues.

Vibrating electrode: removing bubbles by vibration.—Once the problem of oscillations has been solved, there remains the presence of bubbles that do not allow the *Ni* layer to grow. Removing bubbles from the electrode mechanically may be a good option. A vibrating electrode strategy was chosen for this purpose. It is for this reason that a 11000 rpm DC vibrating motor was placed in contact with the composite working electrode. In this way, the $H_2(g)$ formed on the electrode surface due to the reduction of H^+ ions present in the solution were quickly removed from the electrode surface allowing the Ni^{2+} to reach the electrode surface. Furthermore, the vibration promotes the renewal of the solution in contact with the composite surface, thereby facilitating a faster mass transport of electroactive species.

Figure 4A shows the time evolution of mean color intensity and potential during the electroplating experiment with the vibrating electrode. A set of photograms extracted from the video recorded during the experiment were also presented. We observe some differences respect to the non-vibrating electrode. As expected, no bubbles on the electrode surface appear. A more uniform growth of the *Ni* layer on the composite material occurs, commencing at the electrode edges and gradually progressing towards the center of the electrode. In addition, all color signals show smooth lines.

Initially, there is a rapid increase in color intensity, but it diminishes quickly, and by 1500 s, the surface color reverts to its initial state. The changes in variance were also found to be minimal during this 1500 s period (Fig. 4B). One possible reason for the lack of color change in the composite material could be the growth of an internal *Ni* layer within the pores, which does not affect the color. Alternatively, it is possible that a nucleation process is required to initiate the electrodeposition reaction. From these data it is not possible to discern between these or other possibilities. However, looking at the potential curve one can observe no important changes of potential during the first 2000 s if compared with larger times where *Ni* is clearly electrodeposited. Therefore, we can suspect that there is a *Ni* electroreduction process which does not cause an important color change.

We would also like to emphasize the symmetry of the variance peak (Fig. 4B). It has been demonstrated in recent research that the symmetry of the peak is linked to the kinetic mechanism through which the process occurs.[30] The time for which the maximum of the peak appears indicates the time for which half of the analyzed surface is coated and the other half uncovered. This time give us a first indication of the rate of the coating process, however we cannot interpret them in the same way as in a monolayer model, since in that case Ni can be electrodeposited on previously deposited Ni and then, we would observe no change. However, these times are a first indicator of the coating rate, but hardly a measure of the kinetic constant.

In the end, from 6000 s the *Ni* layer just covers the entire surface, and no color change is observed, although *Ni* layer continues growing.

Electrodissolution of Ni.—Once the vibrating electrode has been covered with a *Ni* layer during 7200 s it has been studied the electrodissolution process in two different solutions: one of them with Cl^- anions and the other one with SO_4^{2-} anions.

In the SO_4^{2-} solution, Fig. 5A shows an initial quasi non variation of mean color intensities against the elapsed time, since the first *Ni* layers removed are deposited on *Ni* and no color change was observed. After 1000 s, the decrease of the mean color intensity can be explained by the black surface that appears bellow the "last" *Ni* layer. This is corroborated by the well-defined peak for the time evolution of variance during the stripping experiment (Fig. 5B). The maximum of this peak can be interpreted as the time at which one half of the electrode surface was covered by *Ni* and the other half uncovered, however no information on different film thickness can be extracted from these data. After this time, the variance diminishes, and the mean color intensities eventually reach a state

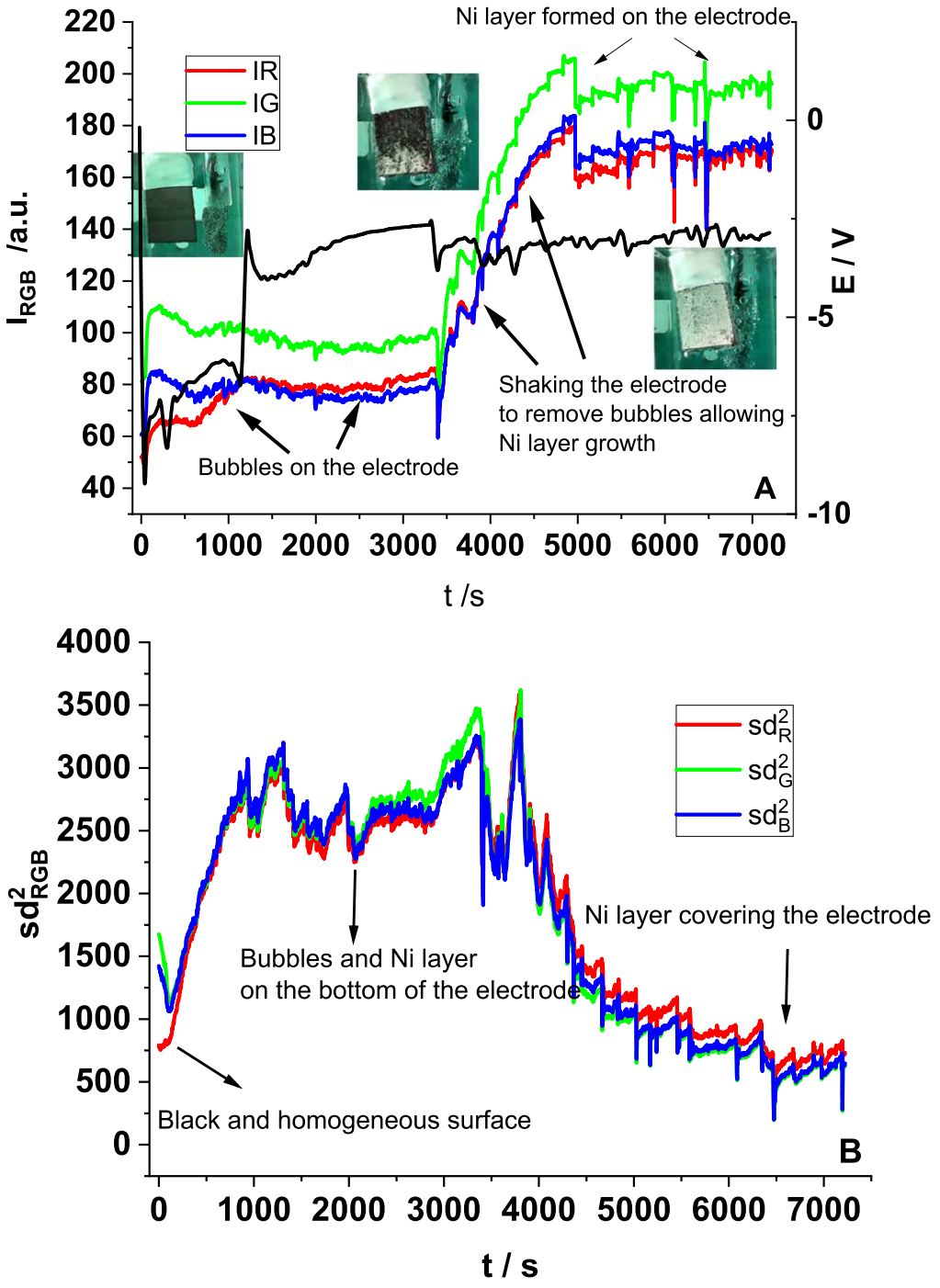

Figure 3. Electrodeposition of Ni without vibration. Galvanostatic experiment with a controlled current of −4 mA in a 245 mM K_2SO_4, 5 mM H_2SO_4 and 100 mM $NiSO_4$ aqueous solution. The auxiliary electrode was behind the composite electrode. (A), mean color intensities and measured potential against the elapsed time. (B) variance of color intensities against the elapsed time. After 3500 s the electrode was periodically shaken to remove bubbles allowing the Ni electrodeposit. Auxiliary electrode was around 1.2 cm behind the working electrode and slightly down.

where no significant alteration takes place (about 2750 s). At this point the variance also proves minimum. After this time and since there is no more *Ni* on the electrode, certain electrochemical reactions linked to the oxidation of the medium occur extensively, causing the appearance of bubbles on the electrode surface and resulting in an increase in variance. Regarding the time evolution of the measured potential during the stripping process, one can observe a potential step during the first seconds, indicating that the electrodissolution of *Ni* has started. At times near 2750 s, where there is no more *Ni* on the electrode surface a potential plateau is observed. This last potential step is explained by the reaction that causes the bubbles on the electrode surface, probably the water oxidation and the oxygen evolution reaction (OER). At this point we can verify that we obtain a similar result if we analyze the evolution of the variance, the color intensity or the electrical potential measured. In all three cases we have times of about 2750 s to completely remove the nickel on the surface of the electrode. Here we can consider an advantage of the image analysis techniques, that is, it allows us to estimate different times on different parts of the electrode, which can lead us to check the homogeneity or not of the electrodeposit.

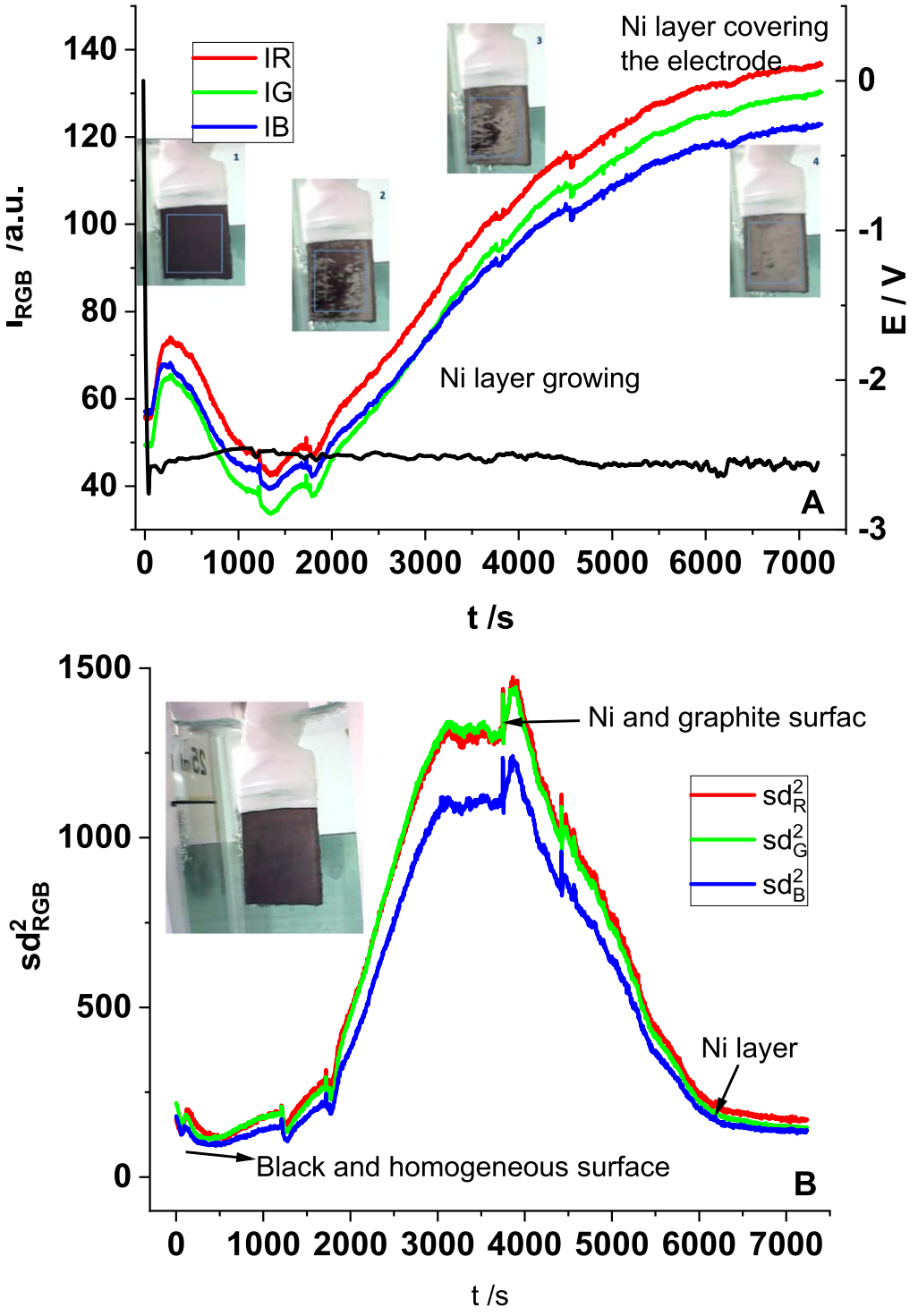

Figure 4. Electrodeposition of Ni on a vibrating electrode. Galvanostatic experiment with a controlled current of −4 mA in a 245 mM K_2SO_4, 5 mM H_2SO_4 and 100 mM $NiSO_4$ aqueous solution. (A) shows the time evolution of mean color intensities and the measured potential, and (B) the time evolution of the mean color variance during the experiment. For more details see the experimental section. The photo in (B) shows the physical disposition of electrodes in the cell (auxiliary electrode behind the working electrode at 1.2 cm).

As observed previously, HER is always present during the nickel electrodeposition. During the electrodissolution in the same aqueous media, there is no other electrochemical reaction than the *Ni* oxidation while *Ni* exists on the electrode and bubbles only appear when there is no more *Ni* on the electrode. Therefore, we can estimate an apparent efficiency of electrodeposition from the time used to cover the composite surface (t_c = 7200 s) and the time needed to remove it (t_r = 2750 s):

$$efficiency(\%) = \frac{t_r}{t_c} \times 100 \quad [3]$$

In these experimental conditions, we estimate an efficiency of about 38%, therefore, a 62% of energy goes to HER.

When we study the electrodissolution process in a chloride-containing medium, we obtain radically different results. Figure 6A.

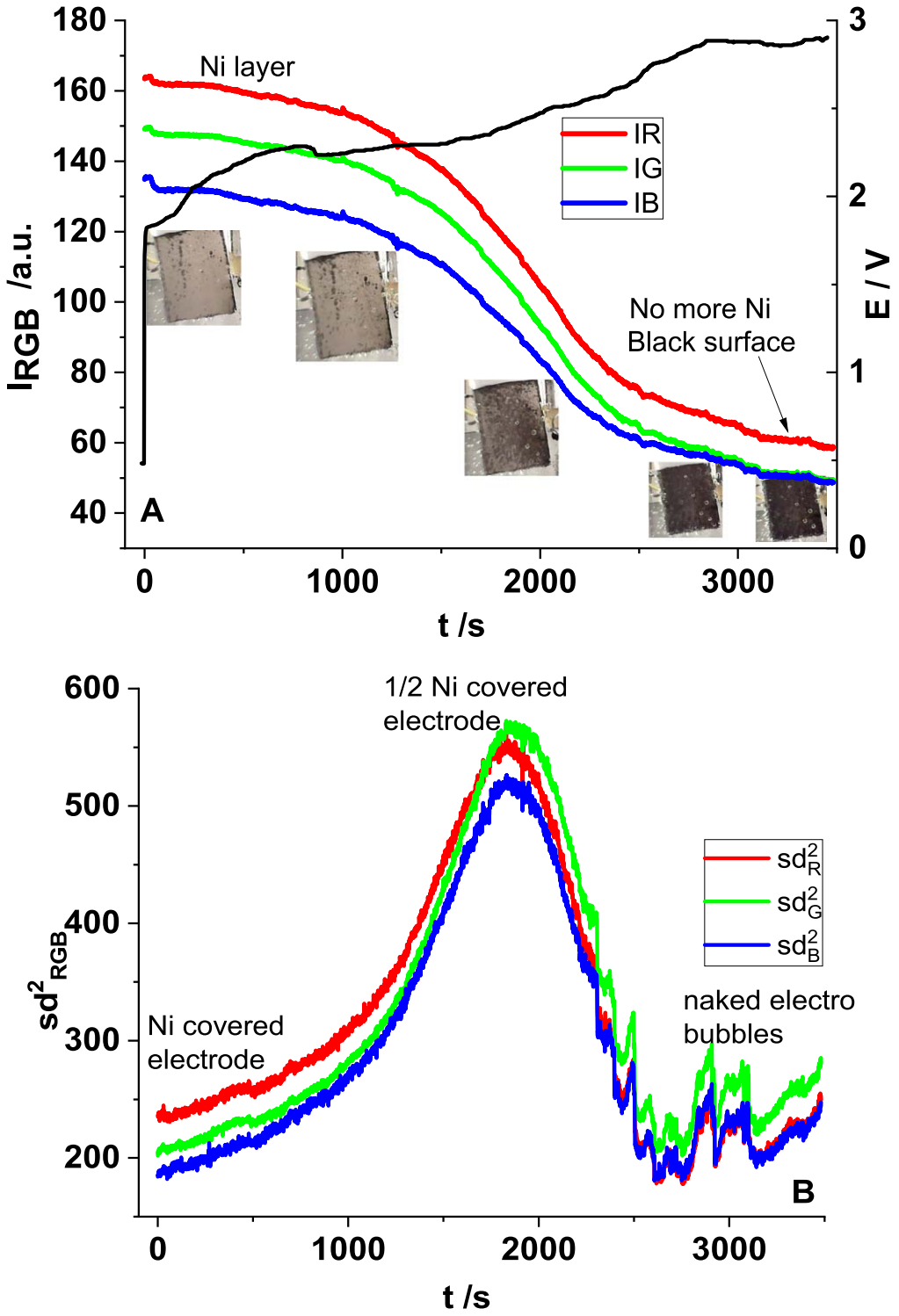

Figure 5. Electrodissolution experiment of the previously formed Ni layer on the electrode. This experiment was carried out in a 10 mM H_2SO_4 and 245 mM K_2SO_4 aqueous solution. Current was controlled to +4 mA. (A) shows the mean color intensities and the measured potential against the elapsed time. (B) shows the variance of color intensities against the elapsed time. Auxiliary electrode was behind the working electrode at 1.2 cm.

On the one side, there is a first increase in the mean color intensity of the electrode surface (about 10–15 RGB units). This first change can be explained by the spontaneous formation of a layer of *Ni* chloride, or the *Ni* oxides or hydroxides compounds helped by the chloride anions adsorption on the electrode surface when this electrode was submerged in the solution containing chloride anions.[40] After, these compounds leave the electrode as the oxidation reaction starts, and the clean *Ni* layer is observed. If this is true, a maximum of variance at these times should be observed as it occurs during the first seconds of the experiment (Fig. 6B). It should be noted that this process takes place only during a few seconds indicating, in any case, the formation of a very thin layer of nickel compounds. After that, the time at which variance proves maximum (1/2 of surface is covered) is about 1100 s, while in the sulphate solution experiment it was about 1800 s. Finally, there is no color change at times larger than 1600 s and in addition, the measured potential also reaches a

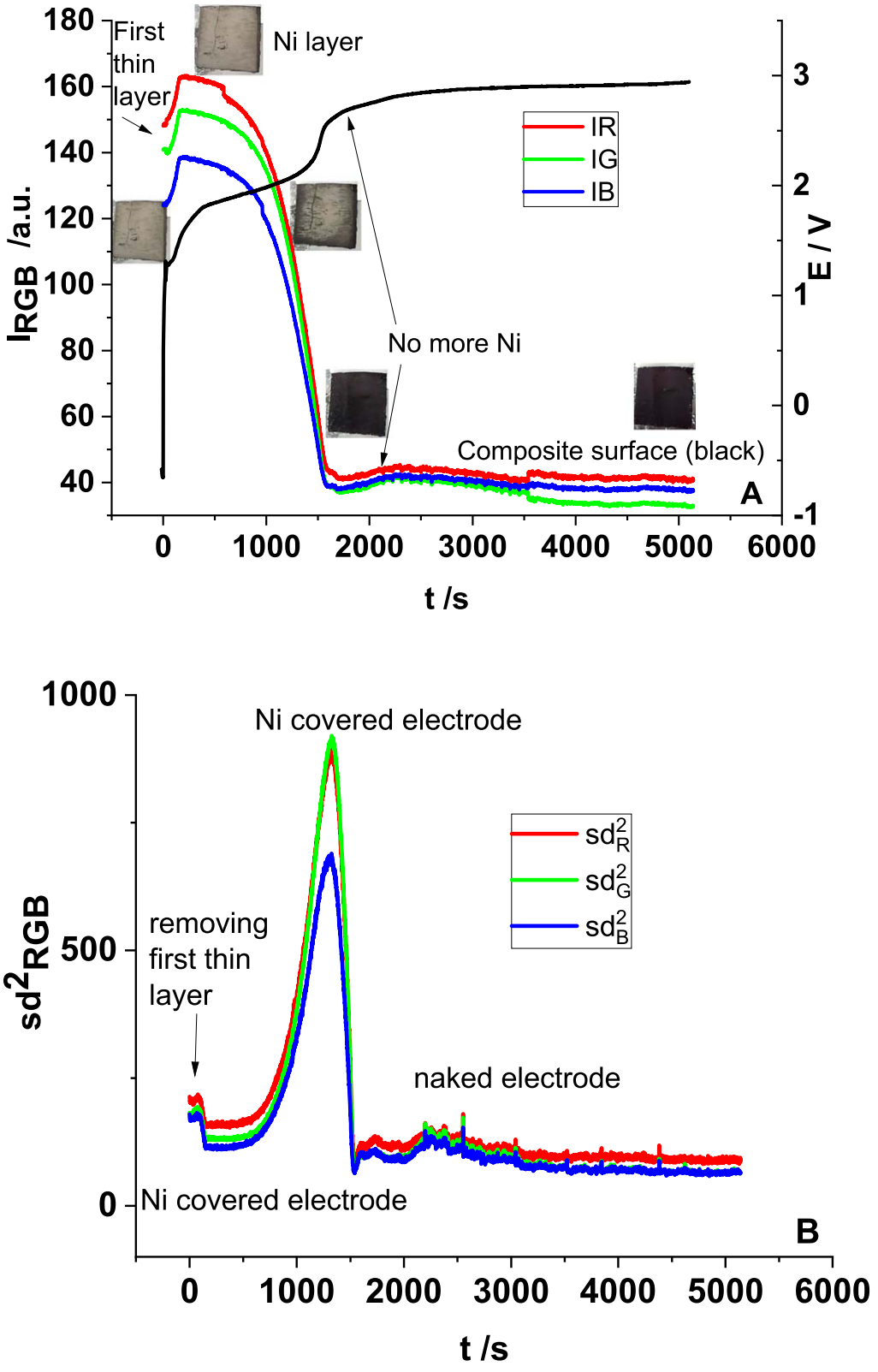

Figure 6. Electrodissolution experiment of the previously formed Ni layer on the electrode. This experiment was carried out in a 1 mM *HCl* and 210 mM *KCl* aqueous solution. Current was controlled to +4 mA. (A) shows the mean color intensities and the measured potential against the elapsed time. (B) shows the variance of color intensities against the elapsed time. Auxiliary electrode was behind the working electrode at 1.2 cm.

constant value after this time since there is no more *Ni*, and the oxidation reactions of the aqueous medium take place on the electrode surface.

In this last case, the apparent efficiency estimated from equation (3) and for the electrodeposition process is only 22%, a very low value if compared with the efficiency estimated from the electrodissolution in a sulphate solution (38%). Since the experimental

conditions for the electrodeposition experiment were identical (solution, current and time), this difference should be attributed to a different electrodissolution mechanism. It has been reported that a non-uniform *Ni* dissolution occurs if large overpotentials or currents are applied in Cl^- containing solutions.[40]

There are at least two possible explanations for this difference. On the one side, *Ni* was oxidized by a chemical attack of hydronium cation since the solution is at pH = 3.0 and in presence of chloride anions. However, this possible reaction should also be considered for the sulphate solution, since the pH was smaller, and more time for the electrodissolution is needed in this last case. A second possible cause for this difference could be a different mechanism for the *Ni* oxidation in both cases. The mechanism for electrodissolution of *Ni* was studied in Cl^- and SO_4^{2-} solutions by cyclic voltammetry, EIS and EQCM.[20,35,41,42] If there are chloride anions in the solution, $Ni(I)$ species were postulated and detected by EIS and EQCM experiments.[21,35] These works expose that the electrodissolution takes place by at least a three steps mechanism: two electron transfer reactions followed by the transport of the oxidized *Ni* to the solution. In other works it has been postulated that nickel can be chemically dissolved by the attack of some anions.[43] What most studies do agree on is that for fast dissolution rates, control by mass transport is a key factor.[44] It is also known that some aggressive anions, such as chloride, destabilize the formation of passive layers.[42,45] In other cases, there is a selection of passivating and non-passivating anions in the solution which marks the rate of the electrodissolution process.[46]

By EQCM analysis, a mass decrease on the electrode surface after *Ni* oxidizes to *Ni*(I) was observed.[35] The second electron transfer takes place without mass changes detected by the EQCM but the current for this reaction is measured. This fact was possible since these EQCM experiments were made without stirring the solution and then *Ni*(I) species can be retained in the interface region. In a vibrating electrode and at very large currents *Ni*(I) species can easier leave the interface, and then the second electron reaction takes place by probably the H^+ participation within the solution and no current associated to this reaction was recorded. On the contrary, $Ni(I)$ species were not detected by EQCM in sulphate solutions and then, *Ni* only leave the electrode/interface region if oxidized to *Ni*(II). That means that *Ni* losses 2 electrons to leave the electrode in non-chloride solutions, but in the presence of chloride anions and thanks to the vibrating electrode, *Ni*(I) species can be removed from the interface, probably as $(NiClOH)^-$,[41] and then chemically oxidized by hydronium cations to $(NiCl)^+_{aq}$. Other authors propose similar mechanisms with $Ni(I)$ species stabilized by chloride anions observing a high electrodissolution rate if the solution was stirred during the experiment [47,48] in good agreement with results here presented. Therefore, assuming that only one electron is required for the electrodissolution process, this hypothesis could be compatible with the different time needed to remove the same layer of *Ni* in SO_4^{2-}(2750 s) and Cl^- solutions (1600 s).

Therefore, and summarizing these possible simplified mechanisms for the electrodissolution in sulphate and chloride solutions two different mechanisms are proposed. In sulphate solutions (Scheme 2), $Ni(I)$ intermediate species are only possible if adsorbed on the electrode surface,[49] but in chloride solutions (Scheme 3) $Ni(I)$ species can pass to the solution stabilized by mixed compounds with chloride anions.[41,47]

At this point, it proves also interesting to analyze the different shape for the variance peaks in a chloride free solution (Fig. 5B and in a chloride solution (Fig. 6B). The first case looks a more symmetrical peak while the second one proves clearly asymmetrical. It has been studied that the shape of these peaks is related with the kinetics order for chemical processes, being symmetrical for zero order kinetics but asymmetrical for first and second order kinetics.[28] In this case the participation of chloride ions from the solution in the electrodissolution process can also explain this behavior.

3D analysis. Spatiotemporal data analysis.—One of the most important advantages of DVEC for the analysis of electrochemical experiments is that this technique allows simultaneously quantifying changes on different parts (regions) of the electrode, that is the spatiotemporal analysis. With the purpose to simplify and for this 3D analysis we only analyze changes for one color (Red) since all three colors show a similar time evolution. It should be noted that in this case, colors change from black (0,0,0) (ideally) to white-grey (200,200,200).

In these experiments, digital video registers what is happening on all the surface of the electrode. The results previously presented refer to the entire electrode surface, but changes cannot take place simultaneously on any part of the electrode surface. The 3D maps will help us interpreting this non-homogeneous behavior. These 3D maps are constructed by analyzing different vertical cuts (10 cuts) of the electrode images at each time. The variable **x** measures the distance from the left side of the electrode as shown in Fig. 7. Figure 8A shows the 3D surface maps of mean red color intensity ($\mathbf{I_R}$) against the elapsed time (**t**) and the distance from the left of the electrode (**x**) during the electrodeposition experiment where oscillations appeared Figs. 2A and 8B is the analogous for the variance of the red color intensity ($\boldsymbol{sd_R^2}$).

Looking at Fig. 8A, one can see that the oscillations (blue horizontal lines) initially take place at any distance, but after 4000 s, when *Ni* starts covering the right side of the electrode, these oscillations are preferably observed far from this region. The amplitude of the oscillations is greater on the right side of the electrode than on the left (15%-20%), as confirmed by Fig. 2B, although in these 3D figures we do not have enough resolution to be able to distinguish these small amplitude changes.

Figure 8A also shows how the *Ni* layer is growing up during the experiment. After 5000 s, it is shown how the covered region does not advance to the left part of the electrode, indicating that *Ni* is only growing on the previously deposited *Ni* layer. Looking now at Fig. 8B, we observe that only on the right side of the electrode a local maximum of variance is reached (1/2 of the surface covered by *Ni*). This maximum is only observed at distances larger than 0.7 cm. In this plot, the covered region is delimited by the curve of maximum variance on the right top of the figure.

It proves interesting comparing this experiment with the analogous electrodeposition with the vibrating electrode (Figs. 8C and

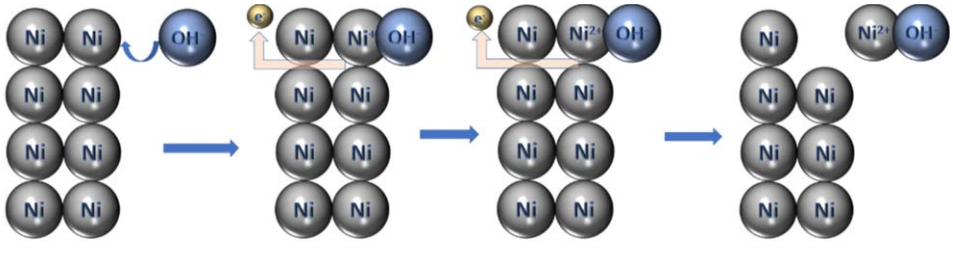

Scheme 2. Possible mechanism of electrodissolution of *Ni* in sulphate containing solutions.[49]

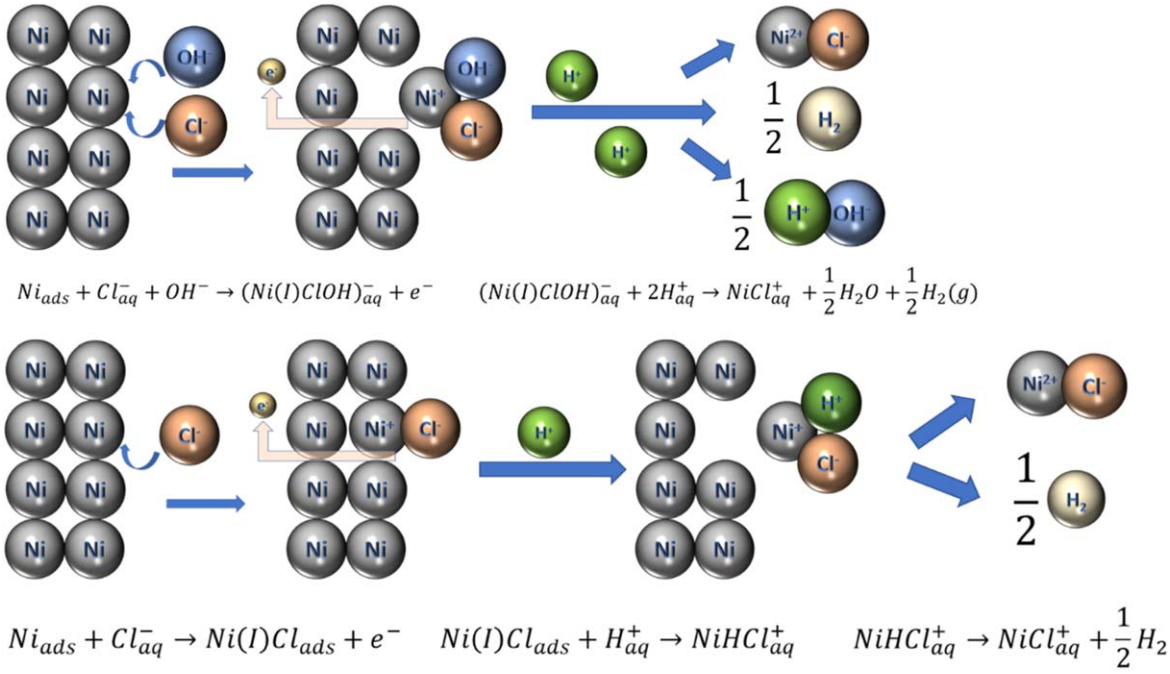

Scheme 3. Possible mechanisms of electrodissolution of *Ni* in chloride containing solutions.[41,47]

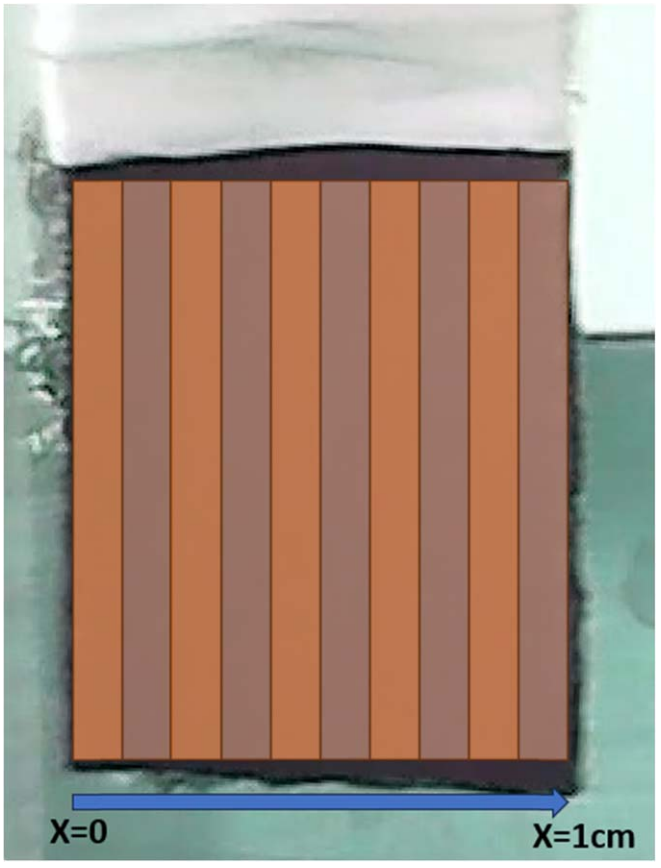

Figure 7. Photogram explaining the preparation of the 3D diagrams. Each vertical section of the electrode surface (10 cuts) is analyzed separately at each instant. The variable x corresponds to the distance from the left side of the electrode surface.

8D). Looking at the mean color intensity (Fig. 8C), one can observe that color evolves more homogeneously that in the non-vibrating electrode case. The right side of the electrode also was the first region in being covered by the *Ni* layer, but in this case differences between the left and the right side are not so pronounced. Variance (Fig. 8D) also shows a more homogeneous growth. The maximum of variance is reached at any part on the electrode surface even when for distances larger than 0.6 cm this time proves smaller. It was also obtained a very homogenous surface after 7200 s since variance reaches new minimum values at all the studied distances. That means that the entire electrode surface was covered by *Ni*. If compared with Fig. 8B, for the non-vibrating electrode, variance proves very different at 7200 s at different parts on the electrode surface. Therefore, these 3D plots can be used as a first quality control of the electrodeposition process.

Conclusions

DVEC allows identifying different issues with the electroplating process and controlling the quality of the final product in situ. Some interesting parameters identifying the rate of the process and the homogeneity of the metal layer can be obtained by the surface image analysis. The time at which variance appears maximum means that one half of the analyzed electrode was covered and could be an excellent parameter to control the quality, homogeneity, and the rate of the electroplating process. This intermediate time can give an extrapolated estimation of the final time needed to get a full covered surface.

The mean color intensities and its time evolution proved as a measure of the surface color at any time and then, a good parameter to evaluate when the process should be stopped. It has also been proved that the presence of bubbles or non-desired processes slowing down the rate of the process can be easily detected during the operation, allowing to correct or to stop the process if necessary. The time evolution of variance should also be used to determine when the entire surface was covered if variance reaches minimum values and a good indicator to extrapolate the final time for the electroplating process. However, if a region of the surface keeps uncovered variance should reach a constant value, but a higher value of this parameter could mean a non-homogeneous electroplated surface.

On the other hand, different times of electrodissolution of the same *Ni* layer in solutions containing sulphate or chloride anions

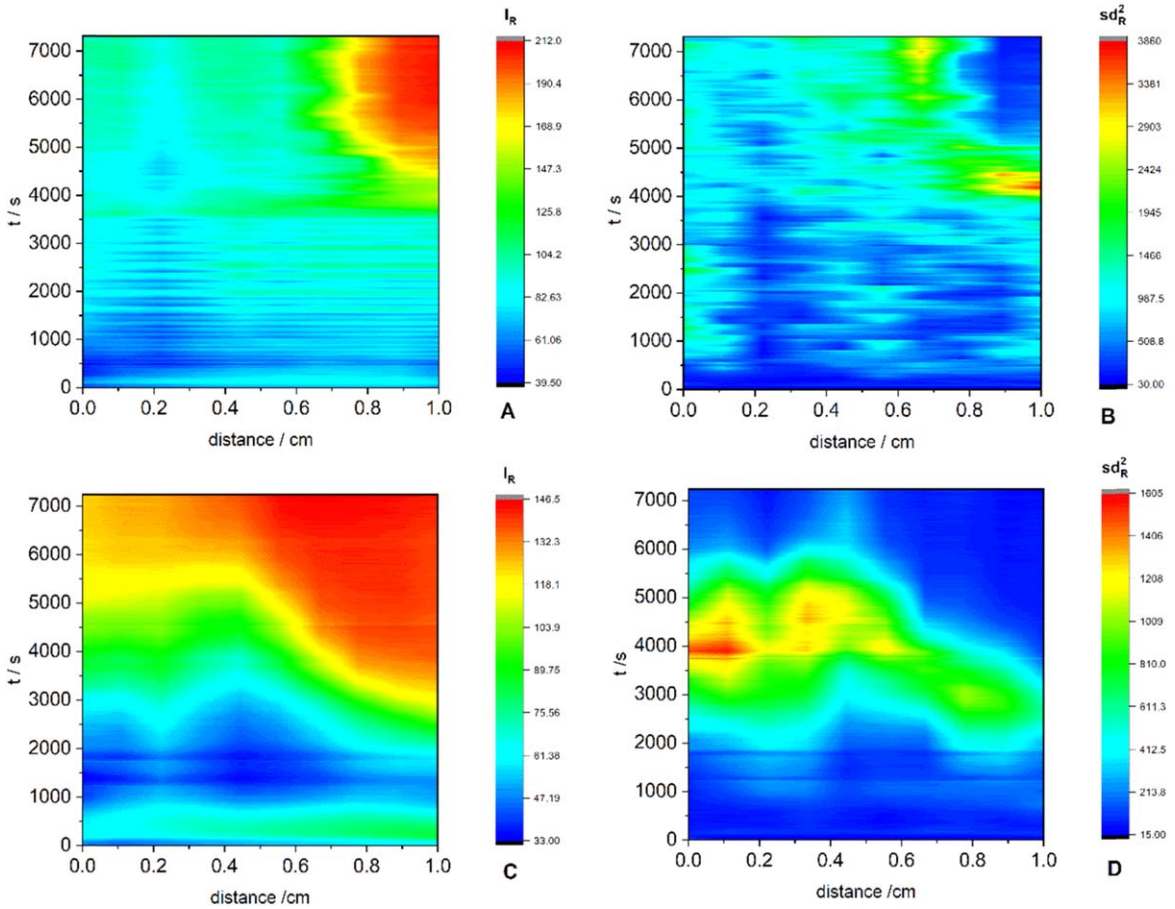

Figure 8. 3D maps of the Red mean color intensity (A) and (C) or the variance of Red color intensity (B) and (D) against the elapsed time and the distance (x) from the left side of the electrode. Electrodeposition of Ni on a non-vibrating electrode and if electrodes are near enough (A) and (B) and on a vibrating electrode (C) and (D). Galvanostatic experiment with a controlled current of −4 mA in a K_2SO_4 0.245 M, H_2SO_4 0.005 M and $NiSO_4$ 0.1 M aqueous solution. (A), the auxiliary electrode was around 0.5 cm on the right of the working electrode. (B), (C) and (D) the auxiliary electrode was behind the working electrode around 1.2 cm.

proved that the dissolution could take place by different mechanisms. In the case of a solution containing chloride anions, *Ni* can leave the electrode surface as a $Ni(I)$ species that should be quickly oxidized by the hydronium cations in the solution. In this case the different times at which the variance reaches minimum values or the time at which mean color intensities keep constant has allowed to propose this different mechanism.

Finally, there is no reason why this technology and methodology could not be extrapolated to the analysis of other processes involving surface color changes or surface homogeneity changes such as it could be the cleaning of surfaces, the growth of biological films on different surfaces, etc.

Acknowledgments

Funding from the Spanish E3TECH-PLUS Research Network (RED2022–134552-T, MICINN/AEI) was acknowledged.

ORCID

Jerónimo Agrisuelas https://orcid.org/0000-0003-0193-2857
José J. García-Jareño https://orcid.org/0000-0002-9247-1314
Francisco Vicente https://orcid.org/0000-0003-1628-918X

References

1. M. A. Reuter, *Metall. Mater. Trans. B*, **47**, 3194 (2016).
2. R. F. van Schalkwyk, M. A. Reuter, J. Gutzmer, and M. Stelter, *J. Clean. Prod.*, **186**, 585 (2018).
3. L. Nazari, C. (Charles) Xu, and M. B. Ray, *Advanced and Emerging Technologies for Resource Recovery from Wastes, Green Chemistry and Sustainable Technology.*, ed. L. Nazari, C. (Charles) Xu, and M. B. Ray (Singapore) (Springer)p. 127 (2021).
4. S. M. Aharoni, *J. Appl. Phys.*, **43**, 2463 (1972).
5. Y. Baziard, S. Breton, S. Toutain, and A. Gourdenne, *Eur. Polym. J.*, **24**, 633 (1988).
6. J. Carratalá-Abril, L. Rey-Martínez, R. Beneito-Ruiz, and J. Vilaplana-Cerdá, *Mater. Today Proc.*, **3**, S240 (2016).
7. J. Navarro-Laboulais, J. Trijueque, J. J. García-Jareño, and F. Vicente, *J. Electroanal. Chem.*, **399**, 115 (1995).
8. Z. Wang, X. Cai, C. Yang, and L. Zhou, *J. Alloys Compd.*, **735**, 905 (2018).
9. X. Sun, H. Sun, H. Li, and H. Peng, *Adv. Mater.*, **25**, 5153 (2013).
10. E. Hammel, X. Tang, M. Trampert, T. Schmitt, K. Mauthner, A. Eder, and P. Pötschke, *Carbon*, **42**, 1153 (2004).
11. Q. Xue, *Eur. Polym. J.*, **40**, 323 (2004).
12. J. Navarro-Laboulais, J. Trijueque, J. J. García-Jareño, and F. Vicente, *J. Electroanal. Chem.*, **422**, 91 (1997).
13. Z. Brito and G. Sanchez, *Compos. Struct.*, **48**, 79 (2000).
14. L. F. Fonseca and I. Balberg, *Phys. Rev. B*, **48**, 14915 (1993).
15. K. Chen, C. Xiang, L. Li, H. Qian, Q. Xiao, and F. Xu, *J. Mater. Chem.*, **22**, 6449 (2012).
16. J. Agrisuelas, J. Garcia-Jareno, M. Piedras, C. Sanz, and F. Vicente, *ECS Trans.*, **50**, 71 (2013).
17. J. Agrisuelas, J. J. García-Jareño, E. Guillén, and F. Vicente, *Electrochim. Acta*, **305**, 72 (2019).
18. J. Agrisuelas, J. J. García-Jareño, E. Perianes, and F. Vicente, *Electrochem. Commun.*, **78**, 38 (2017).
19. M. Schlesinger and M. Paunovic, *Modern Electroplating* (Hoboken, NJ)(Wiley) 5th ed.p. 736 (2014).
20. J. Gregori, J. J. García-Jareño, and F. Vicente, *Electrochem. Commun.*, **8**, 683 (2006).
21. J. Gregori, J. J. García-Jareño, D. Giménez-Romero, and F. Vicente, *Electrochim. Acta*, **52**, 658 (2006).
22. F. Vicente, J. Gregori, J. García-Jareño, and D. Giménez-Romero, *J. Solid State Electrochem.*, **9**, 684 (2005).
23. J. Wang, H. Shao, S. Ren, A. Hu, and M. Li, *Appl. Surf. Sci.*, **539**, 148045 (2021).

24. Z. Shi, S. Wu, S. Lin, J. Sun, H. Huang, D. Kong, Y. Gao, and C. Zhou, *Appl. Surf. Sci.*, **609**, 155250 (2023).
25. W.-S. Kang, W.-C. Chou, W.-J. Li, T.-H. Shen, and C.-S. Lin, *Thin Solid Films*, **660**, 108 (2018).
26. A. Cuenca, J. Agrisuelas, J. J. García-Jareño, and F. Vicente, *Langmuir*, **31**, 12664 (2015).
27. J. Agrisuelas, J. J. García-Jareño, and F. Vicente, *Electrochim. Acta*, **269**, 350 (2018).
28. J. Agrisuelas, J. J. García-Jareño, E. Guillén, and F. Vicente, *J. Phys. Chem. C*, **124**, 2050 (2020).
29. J. Agrisuelas, J. J. García-Jareño, and F. Vicente, *Microchem. J.*, **181**, 107844 (2022).
30. J. Agrisuelas, J. J. García-Jareño, and F. Vicente, *Electrochem. Commun.*, **93**, 86 (2018).
31. Z. Dong and C. Guo, *J. Phys. Conf. Ser.*, **1792**, 012056 (2021).
32. L. N. Ferreira, D. A. Vega-Oliveros, M. Cotacallapa, M. F. Cardoso, M. G. Quiles, L. Zhao, and E. E. N. Macau, *Nat. Commun.*, **11**, 4036 (2020).
33. M. Vidal, J. M. Amigo, R. Bro, F. van den Berg, M. Ostra, and C. Ubide, *Anal. Chim. Acta*, **706**, 1 (2011).
34. M. Vidal, J. M. Amigo, R. Bro, M. Ostra, C. Ubide, and J. Zuriarrain, *Anal. Chim. Acta*, **694**, 38 (2011).
35. J. Gregori, J. Garcia-Jareno, D. Gimenez-Romero, A. Roig, and F. Vicente, *J. Electrochem. Soc.*, **154**, C371 (2007).
36. D. Sazou and M. Pagitsas, *J. Electroanal. Chem. Interfacial Electrochem.*, **312**, 185 (1991).
37. W. Smit and J. G. Hoogland, *Electrochim. Acta*, **16**, 1 (1971).
38. D. Khamis, E. Mahé, F. Dardoize, and D. Devilliers, *J. Appl. Electrochem.*, **40**, 1829 (2010).
39. P. C. Andricacos and H. Y. Cheh, *J. Electrochem. Soc.*, **128**, 838 (1981).
40. G. Dibari, *Plat. Surf. Finish.*, **66**, 76 (1979).
41. S. G. Real, M. R. Barbosa, J. R. Vilche, and A. J. Arvia, *J. Electrochem. Soc.*, **137**, 1696 (1990).
42. M. R. Barbosa, J. A. Bastos, J. J. García-Jareño, and F. Vicente, *Electrochim. Acta*, **44**, 957 (1998).
43. M. Datta and D. Landolt, *Electrochim. Acta*, **25**, 1263 (1980).
44. M. Datta and D. Landolt, *Electrochim. Acta*, **25**, 1255 (1980).
45. R. J. Leese and A. Ivanov, *Adv. Mech. Eng.*, **8**, 1687814015626860 (2016).
46. M. Datta et al., *J. Electrochem. Soc.*, **142**, 3779 (1995).
47. E. E. A. El Aal, W. Zakria, A. Diab, and S. M. A. El Haleem, *J. Mater. Eng. Perform.*, **12**, 172 (2003).
48. E. E. Abd El Aal, *Corrosion*, **55**, 582 (1999).
49. N. Sato and G. Okamoto, *J. Electrochem. Soc.*, **110**, 605 (1963).